TABLE 4-2

ARTS-IIIA/RDAS PROBABILITY OF FALSE TARGET HIT WHEN CONNECTED TO ASR-7 RADAR THAT IS RECEIVING INTERFERENCE FROM ONE RADAR

VICTIM RADAR CHANNEL	INTERFERING RADAR	INTERFERING RATE ν PULSES/SEC	PROBABILITY OF FALSE TARGET HIT (RQT=23)	PROBABILITY OF FALSE TARGET HIT (RQT=24)
NORMAL	ASR-7	1002	0.08026	0.04031
NORMAL	ASR-8	1040	0.08048	0.04011
NORMAL	AN/CPN-4	1192	0.08065	0.04002
NORMAL	AN/FPS-90	356	0.08027	0.04049
NORMAL	WSR-57	166	0.07980	0.03989
MTI	ASR-7	1002	0.08076	0.04087
MTI	ASR-8	1040	0.08143	0.04030
MTI	AN/CPN-4	1192	0.08195	0.04003
MTI	AN/FPS-90	356	0.08077	0.04143
MTI	WSR-57	166	0.07942	0.03932

NOTE: RQT = RANK QUANTIZER THRESHOLD
PROBABILITY OF FALSE TARGET HIT FOR RQT 23 AND NO INTERFERENCE = 0.08
PROBABILITY OF FALSE TARGET HIT FOR RQT 24 AND NO INTERFERENCE = 0.04

TABLE 4-3

ARTS-IIIA/RDAS PROBABILITY OF FALSE TARGET HIT WHEN CONNECTED TO ASR-7 RADAR THAT IS RECEIVING INTERFERENCE FROM THREE RADARS OF THE SAME TYPE

VICTIM RADAR CHANNEL	INTERFERING RADAR	INTERFERING RATE ν PULSES/SEC	PROBABILITY OF FALSE TARGET HIT (RQT=23)	PROBABILITY OF FALSE TARGET HIT (RQT=24)
NORMAL	ASR-7	3006	0.08076	0.04087
NORMAL	ASR-8	3120	0.08143	0.04030
NORMAL	AN/CPN-4	3576	0.08194	0.04003
NORMAL	AN/FPS-90	1068	0.08081	0.04148
NORMAL	WSR-57	498	0.07941	0.03968
MTI	ASR-7	3006	0.08203	0.04213
MTI	ASR-8	3120	0.08418	0.04055
MTI	AN/CPN-4	3576	0.08582	0.03976
MTI	AN/FPS-90	1068	0.08229	0.04424
MTI	WSR-57	498	0.07824	0.03905

NOTE: RQT = RANK QUANTIZER THRESHOLD
PROBABILITY OF FALSE TARGET HIT FOR RQT 23 AND NO INTERFERENCE = 0.08
PROBABILITY OF FALSE TARGET HIT FOR RQT 24 AND NO INTERFERENCE = 0.04

TABLE 4-4

ARTS-IIIA/RDAS PROBABILITY OF FALSE TARGET HIT WHEN CONNECTED TO ASR-8 RADAR THAT IS RECEIVING INTERFERENCE FROM ONE RADAR

VICTIM RADAR CHANNEL	INTERFERING RADAR	INTERFERING RATE ν PULSES/SEC	PROBABILITY OF FALSE TARGET HIT (RQT=23)	PROBABILITY OF FALSE TARGET HIT (RQT=24)
NORMAL	ASR-7	1002	0.07998	0.04046
NORMAL	ASR-8	1040	0.08018	0.04027
NORMAL	AN/CPN-4	1192	0.08031	0.04144
NORMAL	AN/FPS-90	356	0.07968	0.03983
NORMAL	WSR-57	166	0.07985	0.03989
MTI	ASR-7	1002	0.07990	0.04134
MTI	ASR-8	1040	0.08052	0.04076
MTI	AN/CPN-4	1192	0.08090	0.04056
MTI	AN/FPS-90	356	0.07906	0.03949
MTI	WSR-57	166	0.07956	0.03976

NOTE: RQT = RANK QUANTIZER THRESHOLD
PROBABILITY OF FALSE TARGET HIT FOR RQT 23 AND NO INTERFERENCE = 0.08
PROBABILITY OF FALSE TARGET HIT FOR RQT 24 AND NO INTERFERENCE = 0.04

TABLE 4-5

ARTS-IIIA/RDAS PROBABILITY OF FALSE TARGET HIT
WHEN CONNECTED TO ASR-8 RADAR THAT IS RECEIVING
INTERFERENCE FROM THREE RADARS OF THE SAME TYPE

VICTIM RADAR CHANNEL	INTERFERING RADAR	INTERFERING RATE ν PULSES/SEC	PROBABILITY OF FALSE TARGET HIT (RQT=23)	PROBABILITY OF FALSE TARGET HIT (RQT=24)
NORMAL	ASR-7	3006	0.07989	0.04134
NORMAL	ASR-8	3120	0.08052	0.04076
NORMAL	AN/CPN-4	3576	0.08090	0.04056
NORMAL	AN/FPS-90	1068	0.07904	0.03948
NORMAL	WSR-57	498	0.07956	0.03976
MTI	ASR-7	3006	0.07942	0.04359
MTI	ASR-8	3120	0.08140	0.04200
MTI	AN/CPN-4	3576	0.08244	0.04136
MTI	AN/FPS-90	1068	0.07718	0.03848
MTI	WSR-57	498	0.07868	0.03929

NOTE: RQT = RANK QUANTIZER THRESHOLD
PROBABILITY OF FALSE TARGET HIT FOR RQT 23 AND NO INTERFERENCE = 0.08
PROBABILITY OF FALSE TARGET HIT FOR RQT 24 AND NO INTERFERENCE = 0.04

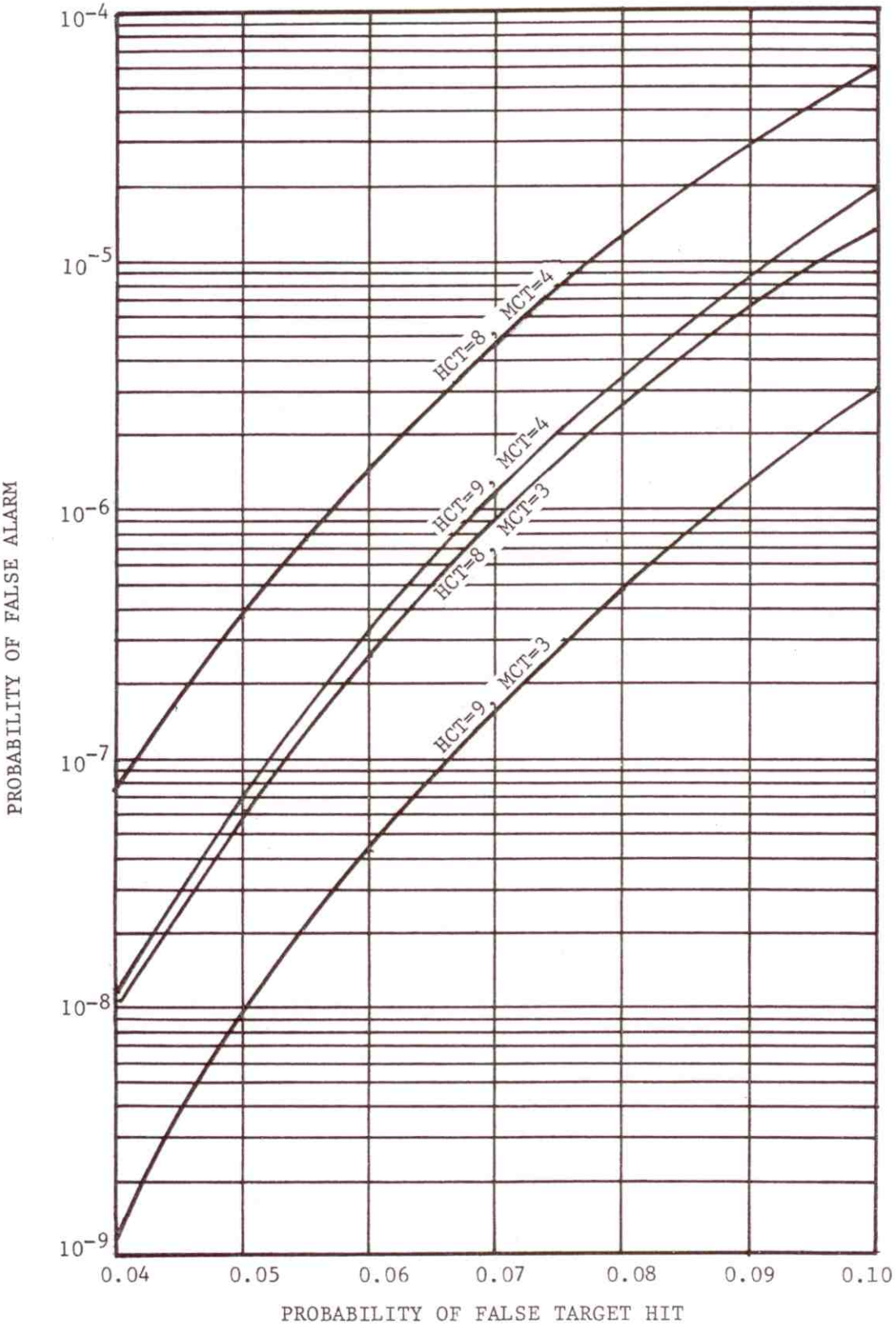

Figure 4-16. ARTS-IIIA/RDAS Probability of False Alarm Versus Probability of False Target Hit for Various Hit/Miss Count Threshold Parameter Combinations

probability of a given sequence is the product of the individual event probabilities, there is a higher probability that the number of noise hits in the sequence will satisfy a lower hit count threshold than a high one.

It is also evident from the curves in Figure 4-16 that raising the consecutive miss count threshold, while maintaining a constant hit count threshold increases the probability of false alarm. Since there is a higher probability of a miss occurring than a hit, due to noise, it is more likely that 4 consecutive misses will occur than 3 consecutive misses and one hit.

The probability of false target hits due to interference shown in TABLES 4-2 through 4-5 were related to the probability of false alarm for a particular hit and miss count threshold by the curves in Figure 4-16. The resulting probability of false alarm values are shown in TABLE 4-6. The probability of false alarms are for the most likely ARTS-IIIA/RDAS parameter settings that will be used in the field:

1. Rank Quantizer Threshold (RQT) = 23

2. Hit Count Threshold (HCT) = 9

3. Miss Count Threshold (MCT) = 3

FAA personnel at NAFEC who have thoroughly tested the ARTS-IIIA are recommending these detection parameter settings be used for optimum performance. In addition, this parameter combination was found in this study (see section on Trade-Off between Interference Suppression and ARTS-IIIA/RDAS Performance) to be near optimum for interference suppression.

The probability of false alarm without interference (4.596×10^{-7}) is shown at the bottom of TABLE 4-6. This number corresponds to a probability of false target hit (0.08) for no interference and a rank quantizer threshold of 23. It is evident from TABLE 4-6 that interfacing the ARTS-IIIA/RDAS to the ASR-7 radar usually results in a higher probability of false alarm than when interfaced to an ASR-8. A higher probability of false alarm also results when the ARTS-IIIA is connected to the MTI channel than the normal channel. The highest probability of false alarm for interfering and victim radar combinations occurred for the AN/CPN-4 and ASR-7. This is because the AN/CPN-4 radar has a higher PRF than any other interfering radar considered. In addition, the probability of an AN/CPN-4 radar pulse falling into a rank quantizer comparison range bin and preventing a hit (logical 1) from being generated by the hit processor is low. This is because the difference between the AN/CPN-4 pulse width (τ_i = 0.5μs) and victim radar range bin hold time (RB_H=0.468μs for ASR-7 versus 0.300μs for ASR-8) is small. It can be seen from Equation 4-3 that a small (τi-RB_H) results in a low value of X_{23} and therefore from Equation 4-6 a high probability of false alarm.

All probability of false alarms for the WSR-57 (τ_i=4.0 μs mode) in TABLE 4-6 are less than for no interference. This is because the WSR-57 wide pulse width cannot overlap the rank quantizer range bin of interest without

TABLE 4-6

ARTS-IIIA/RDAS PROBABILITY OF FALSE ALARM FOR TYPICAL DETECTION PARAMETERS AND VARIOUS COMBINATIONS OF INTERFERING AND VICTIM RADARS

VICTIM RADAR	VICTIM RADAR CHANNEL	NUMBER INTERFERING RADARS OF SAME TYPE	INTERFERING RADAR TYPE				
			ASR-7 τ_i=0.83μs PRF=1002	ASR-8 τ_i=0.60μs PRF=1040	AN/CPN-4 τ_i=0.5μs PRF=1192	AN/CPN-4 τ_i=2.0μs PRF=356	WSR-57 τ_i=4.0μs PRF=166
ASR-7	NORMAL	1	4.914×10^{-7}	5.182×10^{-7}	5.390×10^{-7}	4.926×10^{-7}	4.534×10^{-7}
ASR-7	NORMAL	3	5.524×10^{-7}	6.342×10^{-7}	6.965×10^{-7}	5.585×10^{-7}	4.413×10^{-7}
ASR-7	MTI	1	5.524×10^{-7}	5.182×10^{-7}	6.977×10^{-7}	5.536×10^{-7}	4.417×10^{-7}
ASR-7	MTI	3	7.075×10^{-7}	9.699×10^{-7}	11.702×10^{-7}	7.392×10^{-7}	4.051×10^{-7}
ASR-8	NORMAL	1	4.589×10^{-7}	4.816×10^{-7}	4.975×10^{-7}	4.497×10^{-7}	4.550×10^{-7}
ASR-8	NORMAL	3	4.562×10^{-7}	5.231×10^{-7}	5.695×10^{-7}	4.299×10^{-7}	4.460×10^{-7}
ASR-8	MTI	1	4.565×10^{-7}	5.231×10^{-7}	5.695×10^{-7}	4.305×10^{-7}	4.460×10^{-7}
ASR-8	MTI	3	4.417×10^{-7}	6.305×10^{-7}	7.575×10^{-7}	3.723×10^{-7}	4.187×10^{-7}

NOTE: 1. ARTS-IIIA/RDAS TYPICAL TARGET DETECTION PARAMETERS
RANK QUANTIZER THREHSOLD = 23
HIT COUNT THRESHOLD = 9
MISS COUNT THRESHOLD = 3
2. PROBABILITY OF FALSE ALARM WITHOUT INTERFERENCE = 4.596×10^{-7}

overlapping many comparison range bins. Consequently, there is a very low probability of the range bin of interest having a higher interference signal level than the comparison range bins, which precludes generation of a hit.

Interpretation of Interference Effects on False Alarms

The probability of false alarms shown in TABLE 4-6 can be related to the approximate number of false alarms (false target detection indication on the PPI) per antenna rotation by:

$$FA = PFA \times M \times \frac{PRF \times T}{K} \qquad (4\text{-}9)$$

where

PFA = Probability of false alarm

M = Number of range bins in victim radars radial coverage (1200 for ASR-7 and 1607 for ASR-8)

PRF = Victim Radar Pulse Repetition Frequency (1002 for ASR-7 and 1040 for ASR-8), in pulses per second

T = Victim Radar Antenna Rotation Time (5 seconds assumed for ASR-7 and ASR-8)

K = The average number of azimuth change pulses (ACPs) since initial hit for a probability of false alarm to occur

The average number of ACPs (K) for a false alarm to occur was determined from the program used to compute the probability of false alarm as a function of the probability of a false target hit. The resulting values of K for possible hit and miss count thresholds are given in TABLE 4-7. The probability of false alarms listed in TABLE 4-6 are for a hit and miss count threshold of 9 and 3, respectively. Therefore K=17 was used in Equation 4-9 to relate TABLE 4-6 false alarm probabilities to false alarms per antenna rotation. Evaluating Equation 4-9 for the false alarm probability without interference (4.596×10^{-7}) and the maximum false alarm probability listed in TABLE 7-6 for interference (11.702×10^{-7}) for an ASR-7 victim radar indicates that the number of false alarms per antenna rotation can increase from 0.1625 to 0.41383. This corresponds to an approximate increase from 2 to 5 false alarms every 12 antenna rotations, or 1 additional false alarm every 4 antenna rotations. It should be pointed out that this result reflects extreme worst-case interference conditions. That is, three radars simultaneously and continually interfering over the entire antenna rotation period, and a worst-case interfering radar and victim radar channel combination.

NTIA noted in its 1975 Los Angeles area radar interference measurements (Hinkle, 1976) that FAA radars did not receive interference from more than

TABLE 4-7

AVERAGE NUMBER OF AZIMUTH CHANGE PULSE SINCE INITIAL HIT FOR A FALSE ALARM TO OCCUR

HIT COUNT THRESHOLD (HCT)	MISS COUNT THRESHOLD (MCT)	AVERAGE NO. OF ACPS FOR PFA TO OCCUR (K)
8	3	15
8	4	18
9	3	17
9	4	21

one radar at a given time. In addition, interference coupling in all measurement cases were caused by antenna mainbeam-to-mainbeam or antenna mainbeam-to-backlobe coupling and resulted in interference occurring only over small sectors of the PPI. The maximum false alarm probability listed in TABLE 4-6 for one interfering radar and the ARTS-IIIA connected to the MTI channel is 6.977×10^{-7}.

From Equation 4-9, this corresponds to an increase in false alarms per antenna rotation from 0.1625 to 0.2463, or one additional false alarm every 12 antenna rotations. If interference is received over less than 50 percent of the antenna rotation, due to a single radar or combination of radars interfering one at a time, only one additional false alarm would occur every 24 antenna rotations. It is therefore concluded that present radar interference conditions in congested terminal areas of the U.S. would not significantly affect the ASR-7 or ASR-8 probability of false alarm when these radars are interfaced to the ARTS-IIIA/RDAS.

The hit count threshold of 9 used in the false alarm analysis corresponds to only the lowest hit count threshold value that the MTI channel can have at any given time. As discussed in a previous section and described in Figure 4-7, the MTI channel hit count threshold is increased from 8 to a maximum of 20 depending on the degree of clutter correlation. The probability of false alarm versus probability of false target hit curves in Figure 4-16 have nearly the same slope regardless of the hit count threshold. Therefore, it is reasonable to assume that an increase in the MTI target hit count threshold would not result in interference having any greater impact than indicated in TABLE 4-6.

Effect of Interference on Probability of Target Detection

The following discusses the impact of interference on the RDAS probability of target detection. The probability of target detection is defined as the probability of declaring a target when the target is actually present. For a target to be declared, a sequence of hits (logical 1) due to target return pulses must be generated by the hit processor in the same range bin for adjacent ACPs, and the target declaration hit and miss count threshold in the target detection software satisfied. Therefore, to analytically determine the probability of target detection, the probability of a target hit at the hit processor output for the target and interference signal are first determined, and then related to probability of target detection through simulation of the target detection criteria. The last portion of this subsection discusses the interpretation of the results.

Probability of Target Hit Caused by a Target

The probability of a logical 1 occurring at the Hit Processor output when a target is present is defined as the probability of a target hit and derived in Appendix F to be:

$$P_{sl}(J,RQT) = \int_{-\infty}^{+\infty} \sum_{K=RQT}^{J} \binom{J}{K} [F(v)]^K [1-F(v)]^{J-K} d[G(v)] \qquad (4\text{-}10)$$

where

v = Voltage level, in volts

J = Number of rank quantizer comparison range bins (24)

RQT = Rank quantizer threshold (23 or 24)

F(v) = Statistical cumulative distribution for noise

G(v) = Statistical cumulative distribution for signal-plus-noise

The probability of target hit (PTH), unlike the probability of false target hit, is dependent not only on the distribution of noise but also the signal-plus-noise distribution. Equation 4-10 gives the probability of the target range bin (range bin of interest with target in it) having a voltage level greater than at least RQT of the surrounding J comparison range bin noise samples. These noise range bins are assumed to each have the same cumulative distribution F(v). The particular distributions for F(v) and G(v) depends on the radar channel (normal or MTI) connected to the ARTS-IIIA/RDAS.

Normal Channel. The noise distribution at the radar normal channel output (before integrator) is Rayleigh distributed (Skolnik, 1962) and given by:

$$F(v) = 1-e^{-v^2/2} \qquad (4\text{-}11)$$

Where v is a sample of the voltage amplitude. The cumulative distribution for signal-plus-noise at the radar normal channel output is given by the Rice distribution (Skolnik, 1962):

$$G(v) = \int_0^v t\, e^{-\frac{t^2+2\cdot SNR}{2}} I_o(t\sqrt{2\cdot SNR})\, dt \qquad (4\text{-}12)$$

t = Dummy variable of integration

SNR = Signal-to-noise voltage ratio

I_o = Modified Bessel function of the first kind and of zero order

Substituting F(v) and G(v) into Equation 4-10 gives:

$$P_{sl}(J,RQT) = \int_0^{+\infty} \sum_{K=RQT}^{J} \binom{J}{K} \left(1-e^{-\frac{v^2}{2}}\right)^K \left(e^{-\frac{v^2}{2}}\right)^{J-K} v\, e^{-\frac{v^2+2\cdot SNR}{2}} I_o(v\sqrt{2\cdot SNR})\, dv \qquad (4\text{-}13)$$

For a rank quantizer threshold (RQT=23) and range bin sample number (J=24), Equation 4-13 becomes:

$$P_{s1}(24,23) = 24\int_0^{\infty}(1-e^{-\frac{v^2}{2}})^{23}(e^{-\frac{v^2}{2}})v\,e^{-\frac{v^2+2\cdot SNR}{2}}I_o(v\sqrt{2\cdot SNR})\,dv + \int_0^{\infty}(1-e^{-\frac{v^2}{2}})^{24}v\,e^{-\frac{v^2+2\cdot SNR}{2}}I_o(v\sqrt{2\cdot SNR})\,dv \qquad (4\text{-}14)$$

Evaluation of Equation 4-13 for a rank quantizer threshold of 24 gives:

$$P_{s1}(24,24) = \int_0^{\infty}(1-e^{-\frac{v^2}{2}})^{24}v\,e^{-\frac{v^2+2\cdot SNR}{2}}I_o(v\sqrt{2\cdot SNR})\,dv \qquad (4\text{-}15)$$

The two above integral equations were evaluated for various signal-to-noise ratios (SNRs) using a Fortran numerical integration routine. The resulting curves are shown plotted on probability paper in Figure 4-17. The probability of target hit curves for RQT=23 is higher than for RQT=24 because there is a higher probability of the signal-plus-noise level in the target range bin exceeding 23 range bin noise samples than 24. Since the distribution of noise and signal-plus-noise out of the ASR-7 and ASR-8 radar normal channel are identical, the curves in Figure 4-17 apply to an ARTS-IIIA/RDAS connected to either an ASR-7 or ASR-8 radar normal channel.

MTI Channel. The ASR-7 has a single channel MTI canceller, and the ASR-8 has a dual (Inphase and Quadrature) MTI canceller. The probability of a target hit with the ARTS-IIIA/RDAS connected to these circuits was computed by the following form of Equation 4-10.

$$P_{s1}(J,RQT) = \int_{-\infty}^{+\infty}\sum_{K=RQT}^{J}\binom{J}{K}[F(v)]^K[1-F(v)]^{J-K}\frac{d[G(v)]}{dv}dv \qquad (4\text{-}16)$$

where d[G(v)]/dv is the signal-plus-noise amplitude distribution PDF.

The noise only amplitude distribution PDF at the output of the ASR-7 MTI channel is a one-sided Gaussian and described by Equation C-40. Therefore, the noise only cumulative distribution is given by:

$$F(v) = \frac{2}{\sqrt{2\pi}\,\sigma}\int_0^V e^{-v^2/2\sigma^2}dv = 2ERF(v) \qquad (4\text{-}17)$$

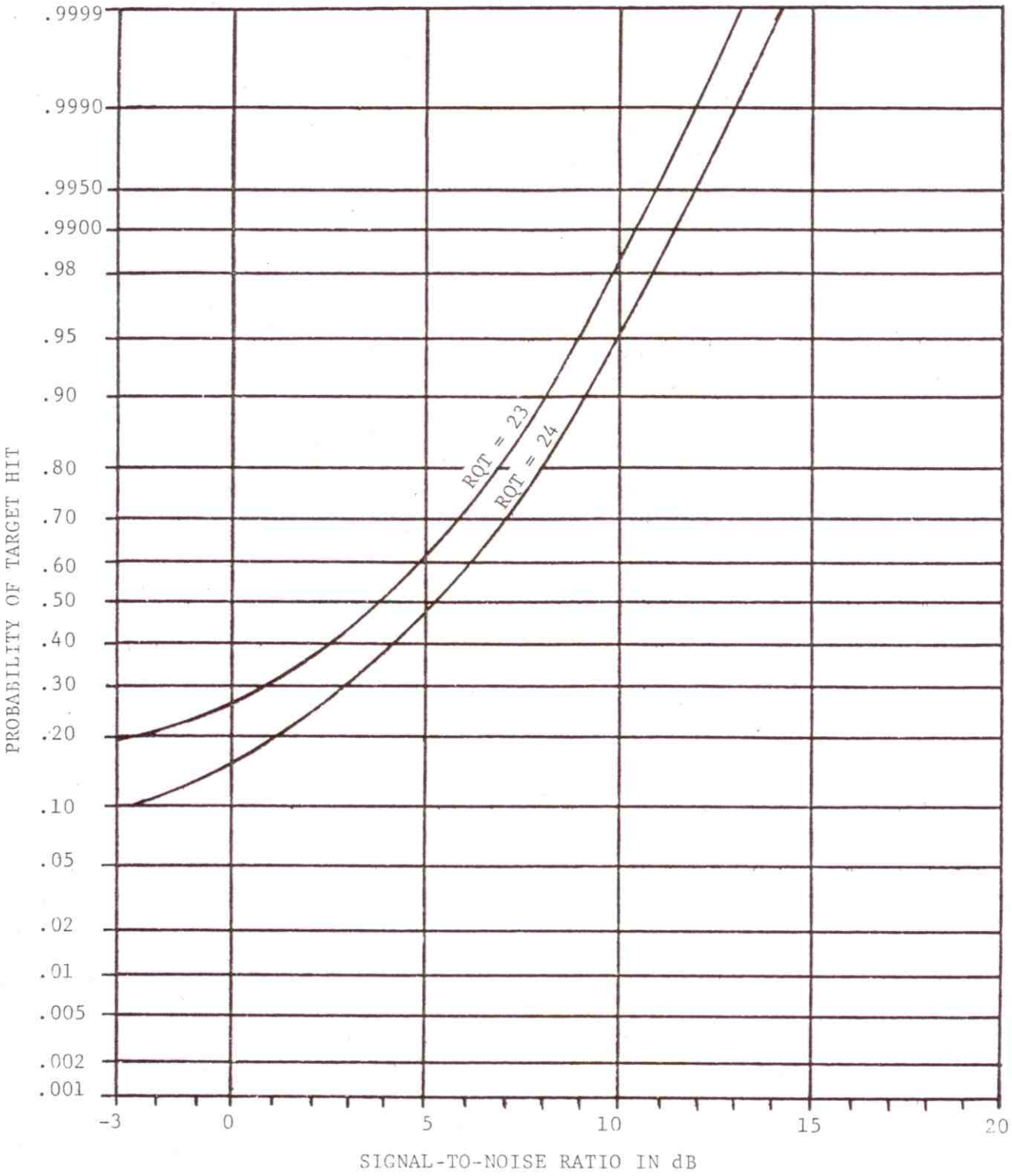

Figure 4-17. Probability of Target Hit Versus Signal-to-Noise Ratio for the ARTS-IIIA/RDAS Connected to the ASR-7 or ASR-8 Radar Normal Channel (Rank Quantizer Threshold 23 and 24)

where ERF(v) is the mathematical error function. The signal-plus-noise amplitude distribution PDF was determined from actual ASR-7 radar MTI channel simulations and is shown in Figure C-21. The probability of a target hit occurring was computed by substituting Equation 4-17 for F(v) in Equation 4-16, and the density distribution data obtained from simulations for d[G(v)]/dv in Equation 4-16. Equation 4-16 was then evaluated for various signal-to-noise ratios (SNR's) using Fortran error function and numerical integration routines. The resulting probability of target hit versus signal-to-noise ratios are shown plotted on probability paper in Figure 4-18.

The noise only amplitude distribution PDF at the ASR-8 MTI Channel output is Rayleigh distributed and given by Equation D-15. Therefore, the noise only cumulative distribution is given by:

$$F(v) = 1 - e^{-v^2/2\sigma^2} \qquad (4\text{-}18)$$

As in the case of the ASR-7 MTI channel, the ASR-8 MTI channel was simulated to determine its output signal-plus-noise amplitude distribution PDF. The resulting density function, shown in Figure C-23, was substituted for d[G(v)]/dv in Equation 4-16. Similarly, Equation 4-18 was substituted for F(v) in Equation 4-16. Equation 4-16 was then evaluated for various signal-to-noise ratios (SNR's) by a numerical integration routine. The resulting probability of target hit versus signal-to-noise ratios are shown plotted in Figure 4-19. The RMS noise voltage level (σ) was set at 0.25 volts for the calculation, since this corresponds to the one volt peak noise level usually set at the radar receiver output.

Interference Effect on Target Hit

A 0.7 probability of target hit was chosen for a zero interference reference base in the analysis. It will be shown later in this section that this probability of target hit results in a worst-case interference effect on probability of target detection. It is evident from Figures 4-17, 4-18, and 4-19 that a 0.7 probability of target hit and RQT=23 corresponds to a signal-to-noise ratio of approximately 6 dB for the ARTS-III/RDAS connected to the normal channel, 12 dB for the ASR-7 MTI channel, and 7 dB for the ASR-8 MTI channel. The effect of interference on the probability of false target hit can be determined from Equation 4-1. As discussed earlier, for worst-case interfering signal level assumptions Equation 4-1 defines the effect of interference on a hit (logical 1) caused by either noise or signal-plus-noise. Substituting 0.7 for P_1 in Equation 4-1 and evaluating it for various interfering pulse arrival rates (ν), gives the curves shown in Figures 4-20 through 4-27. The graphs in Figures 4-20 through 4-23 are for

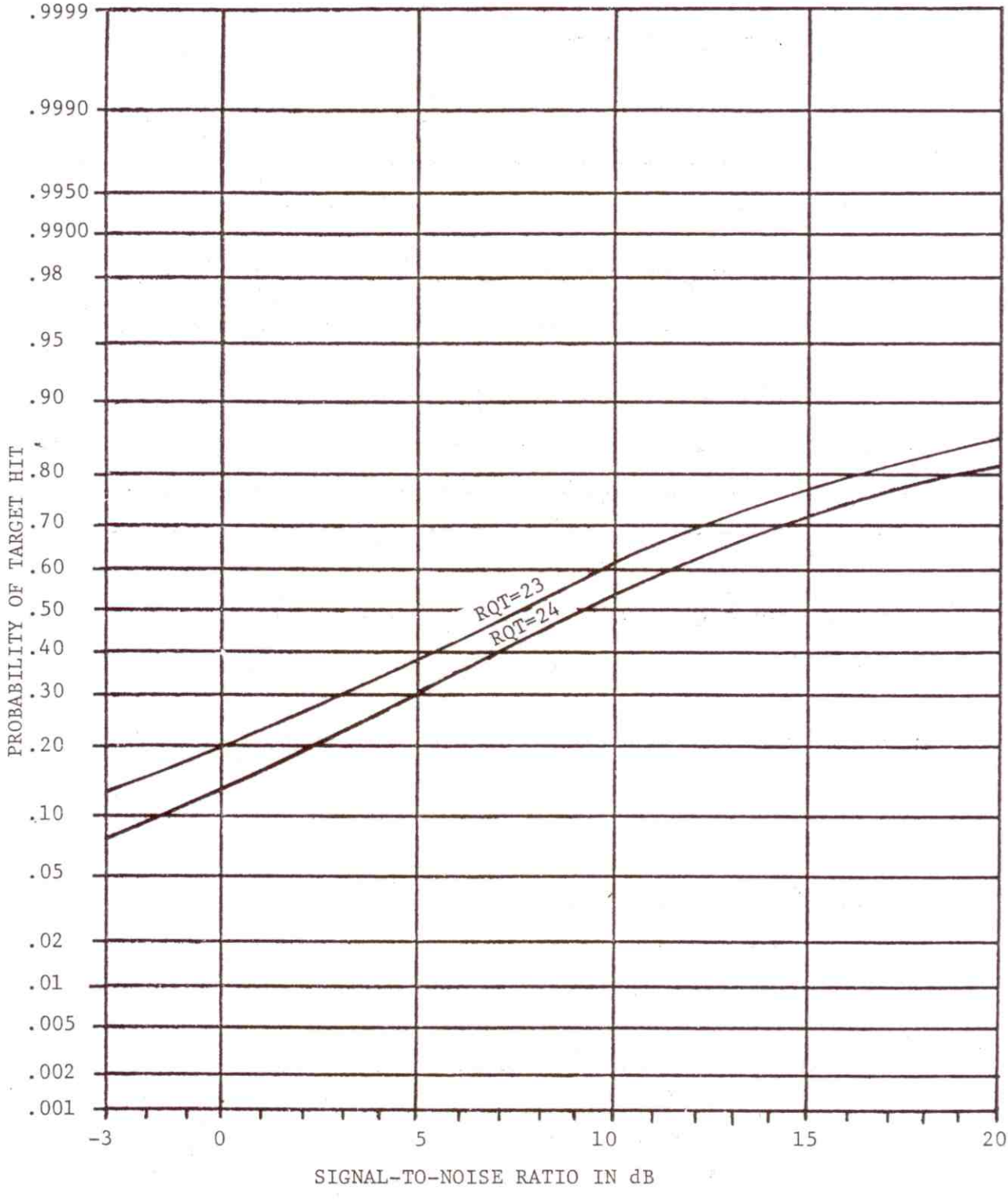

Figure 4-18. Probability of Target Hit Versus Signal-to-Noise Ratio for the ARTS-IIIA/RDAS Connected to the ASR-7 Radar MTI Channel (Rank Quantizer Threshold 23 and 24)

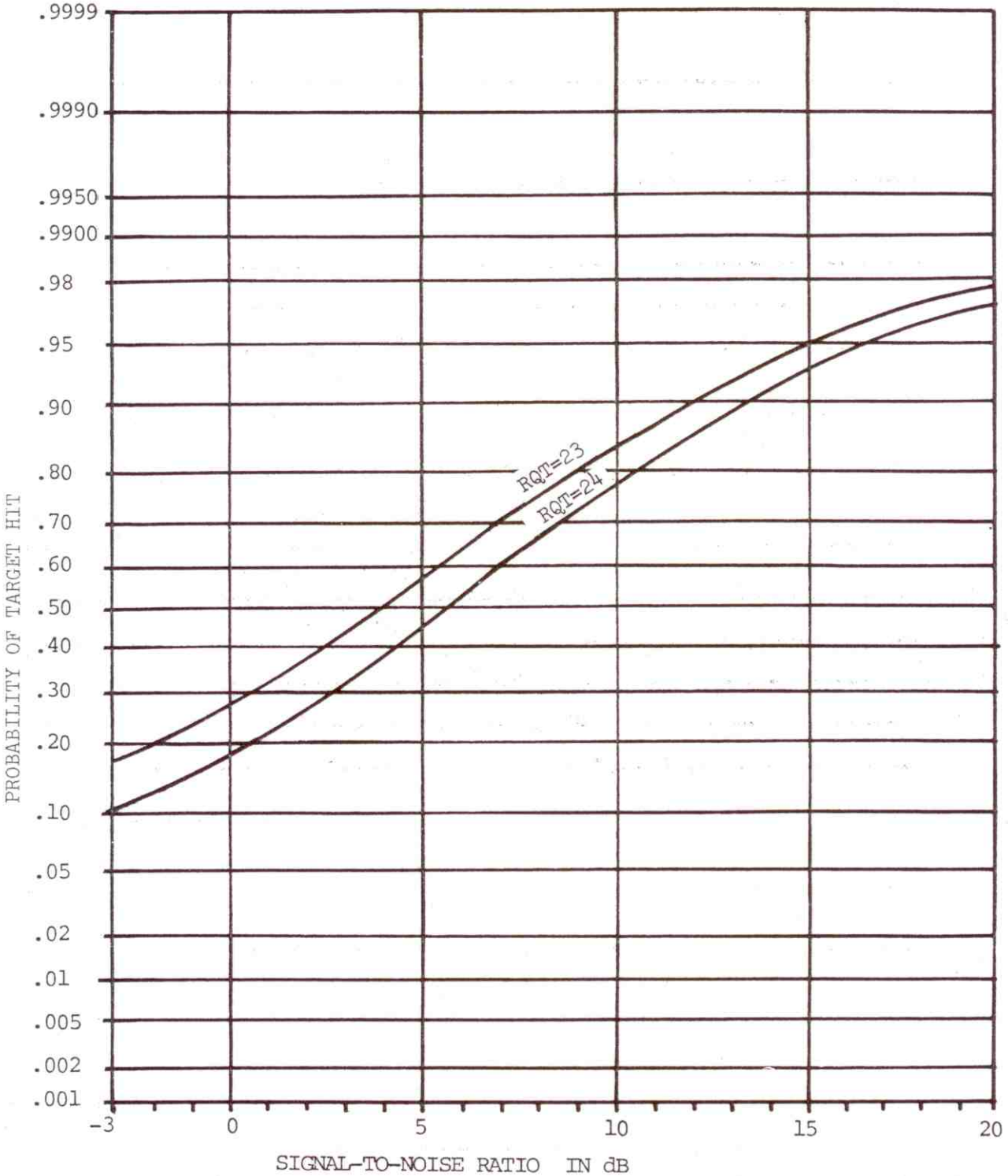

Figure 4-19. Probability of Target Hit Versus Signal-to-Noise Ratio for the ARTS-IIIA/RDAS Connected to the ASR-8 Radar MTI Channel (Rank Quantizer Threshold 23 and 24)

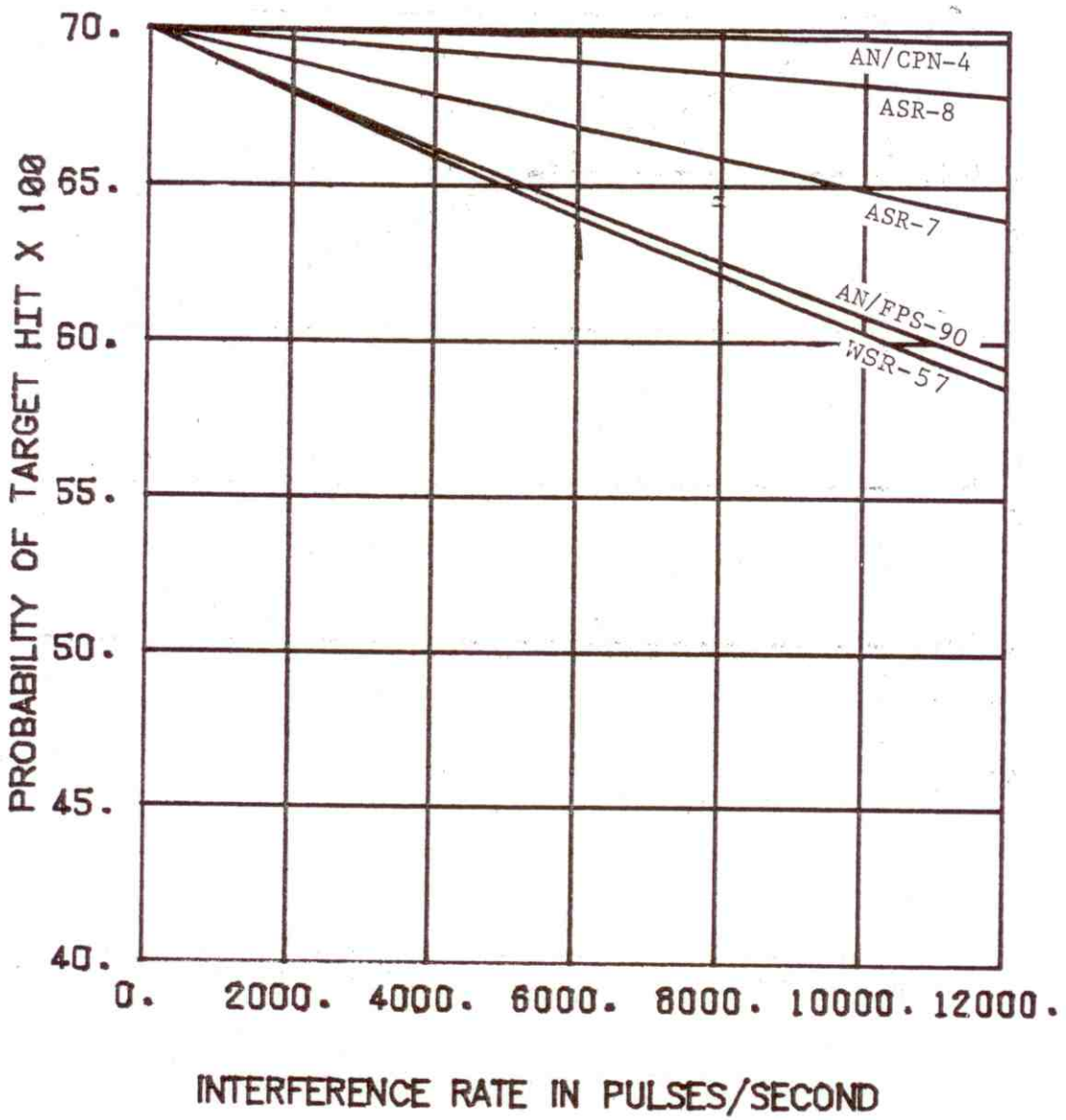

Figure 4-20. ARTS-IIIA/RDAS Probability of Target Hit Versus Rate of Received Interference (ASR-7 Victim Radar, Normal Channel, Rank Quantizer Threshold 23)

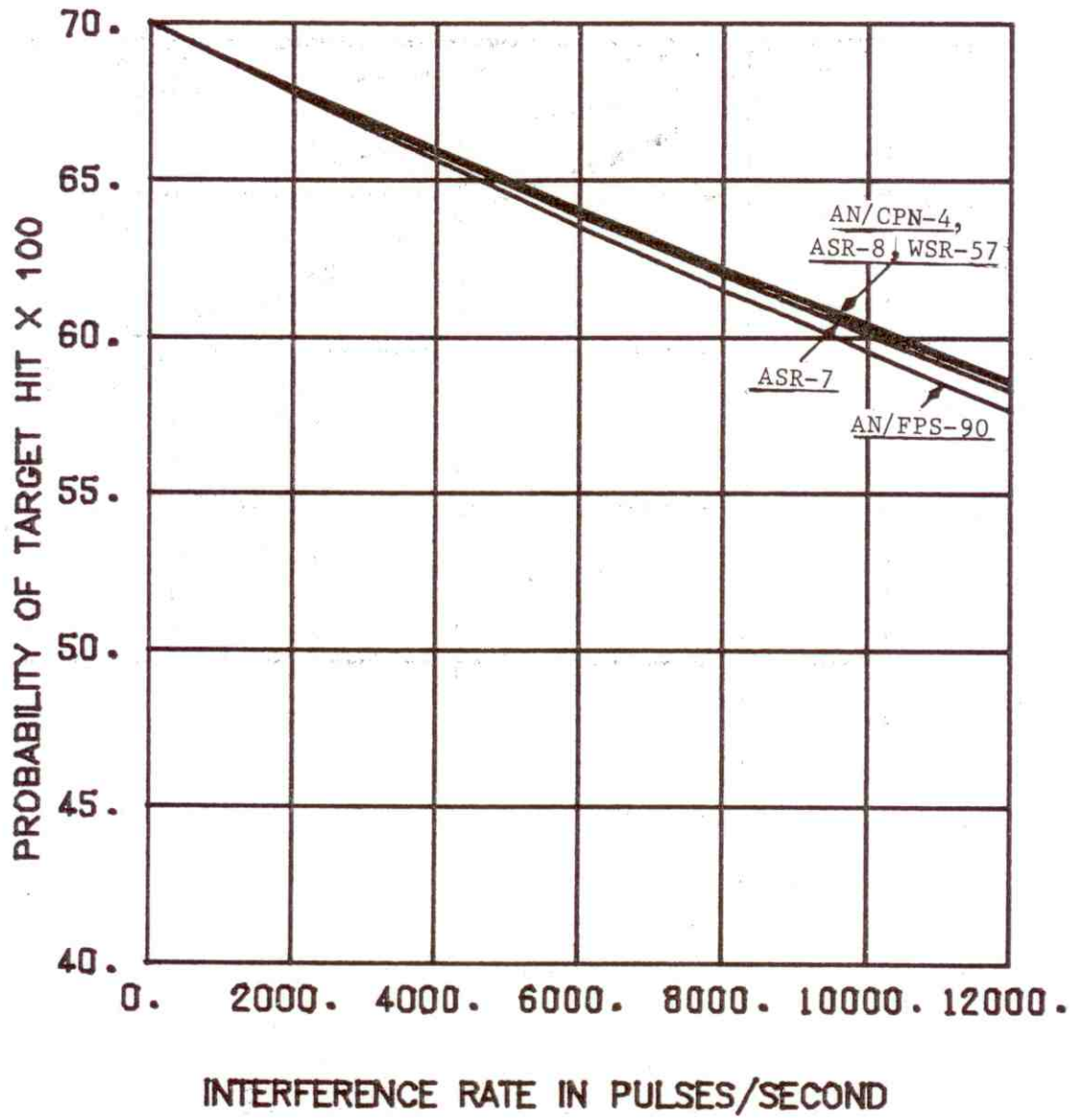

Figure 4-21. ARTS-IIIA/RDAS Probability of Target Hit Versus Rate of Received Interference (ASR-7 Victim Radar, Normal Channel, Rank Quantizer Threshold 24)

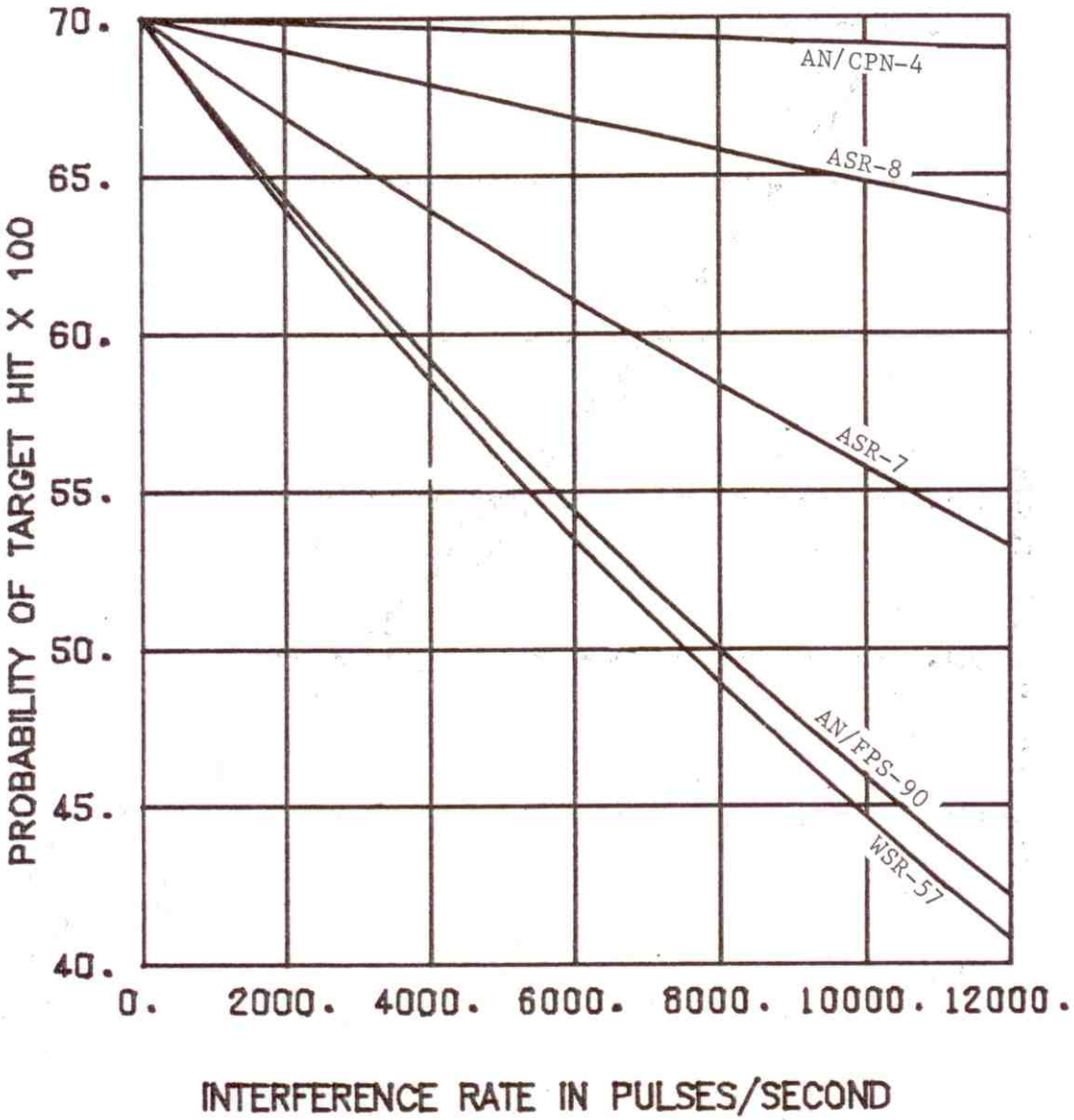

Figure 4-22. ARTS-IIIA/RDAS Probability of Target Hit Versus Rate of Received Interference (ASR-7 Victim Radar, MTI Channel, Rank Quantizer Threshold 23)

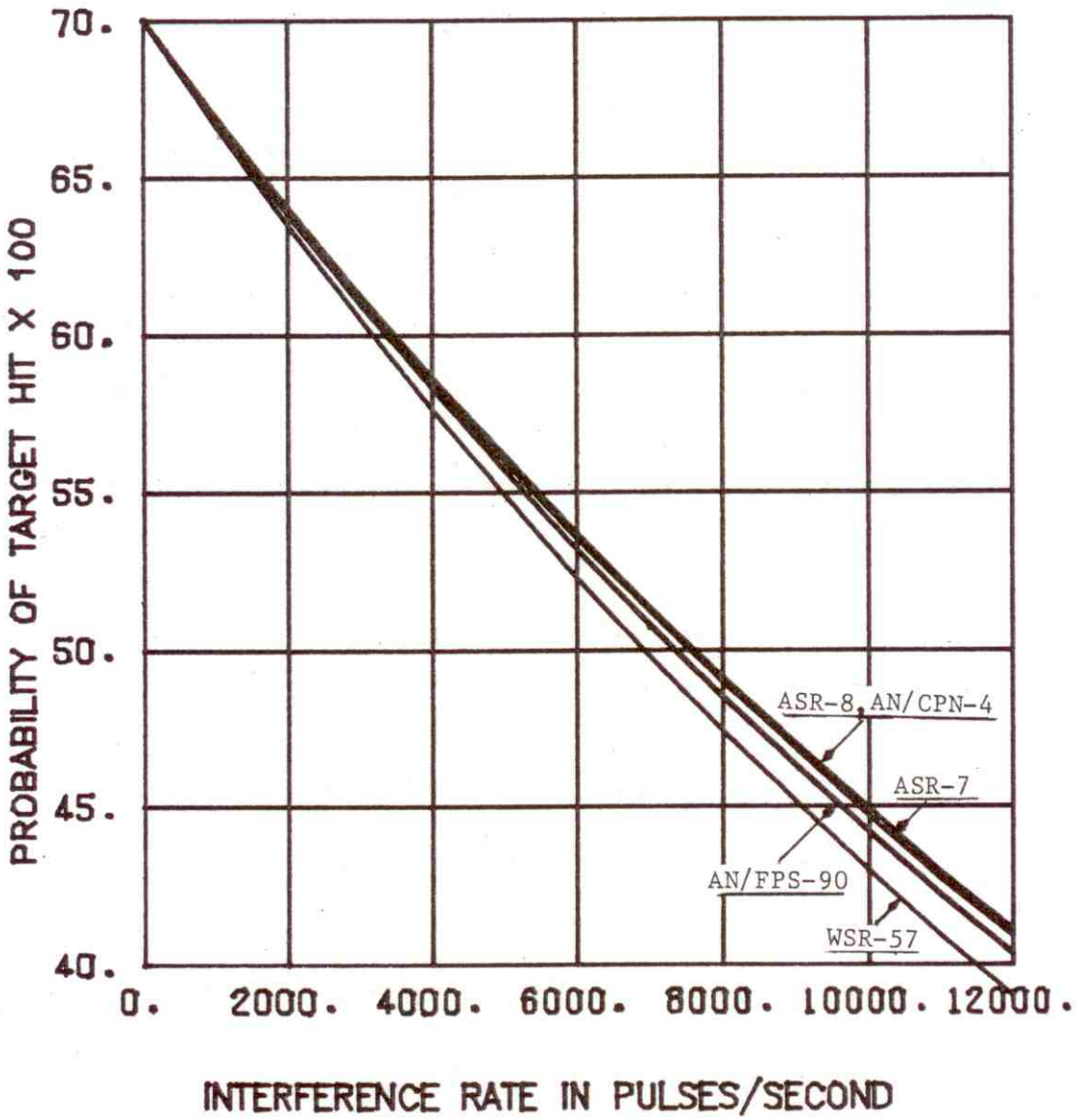

Figure 4-23. ARTS-IIIA/RDAS Probability of Target Hit Versus Rate of Received Interference (ASR-7 Victim Radar, MTI Channel, Rank Quantizer Threshold 24)

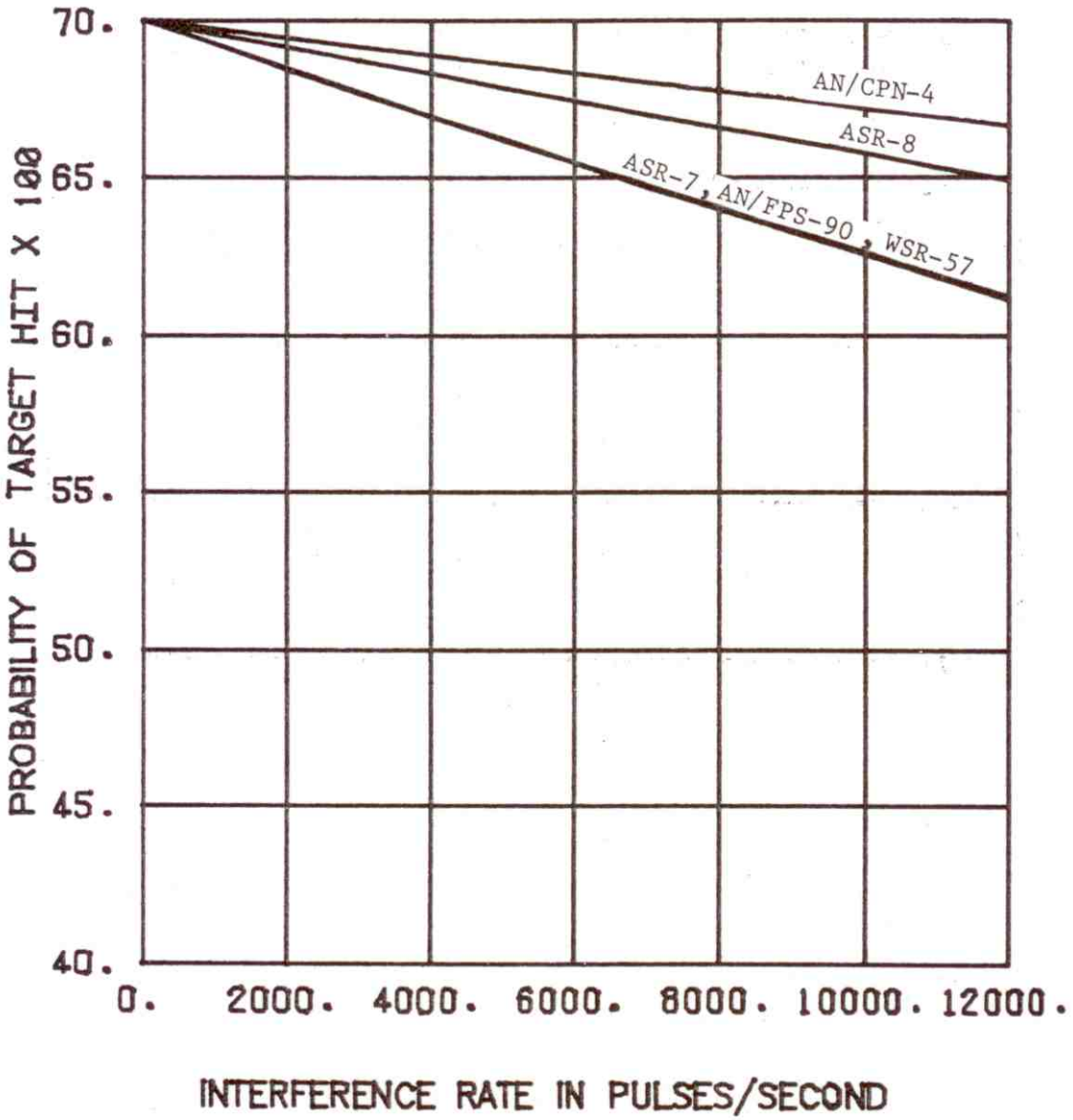

Figure 4-24. ARTS-IIIA/RDAS Probability of Target Hit Versus Rate of Received Interference (ASR-8 Victim Radar, Normal Channel, Rank Quantizer Threshold 23)

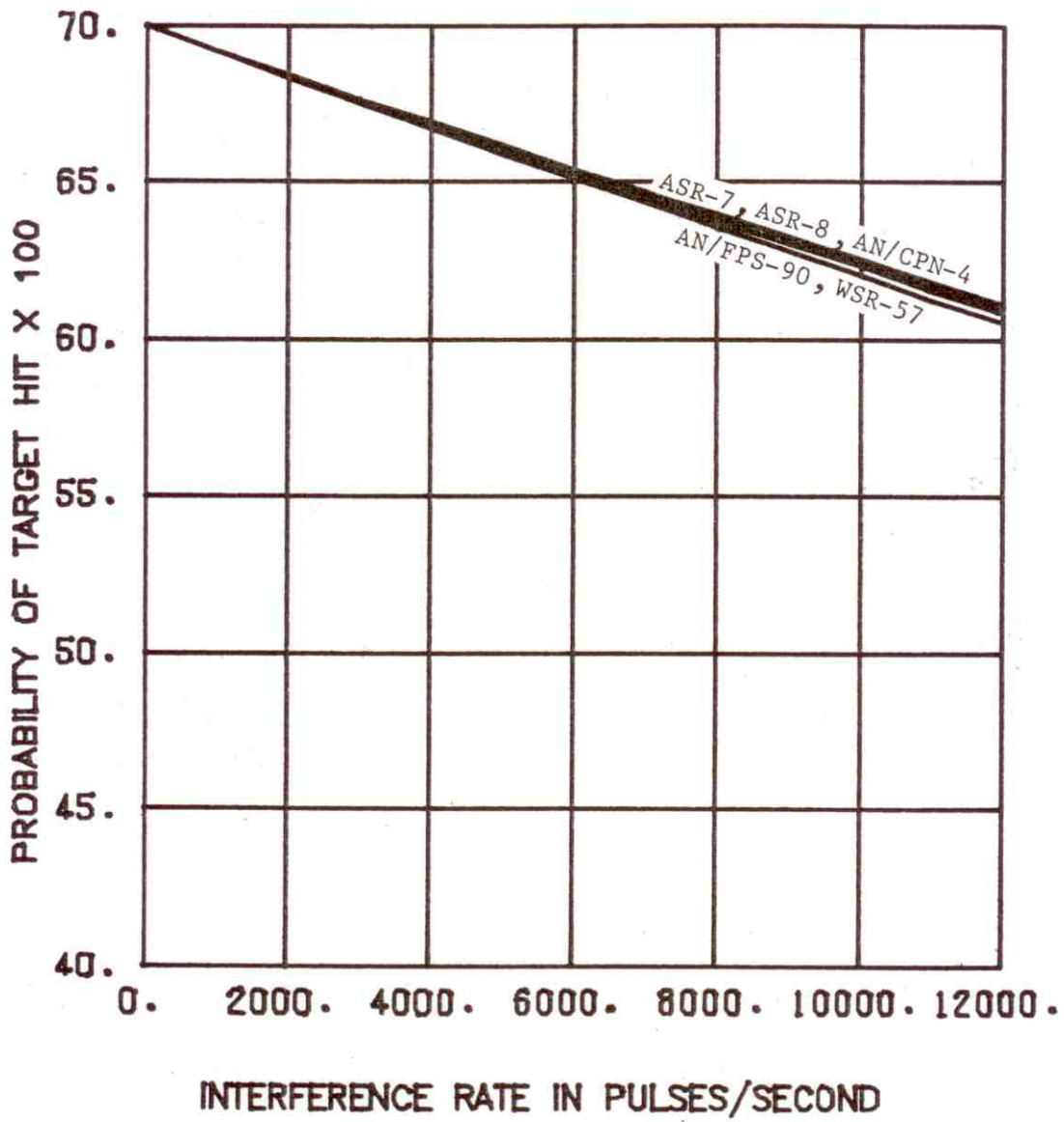

Figure 4-25. ARTS-IIIA/RDAS Probability of Target Hit Versus Rate of Received Interference (ASR-8 Victim Radar, Normal Channel, Rank Quantizer Threshold 24)

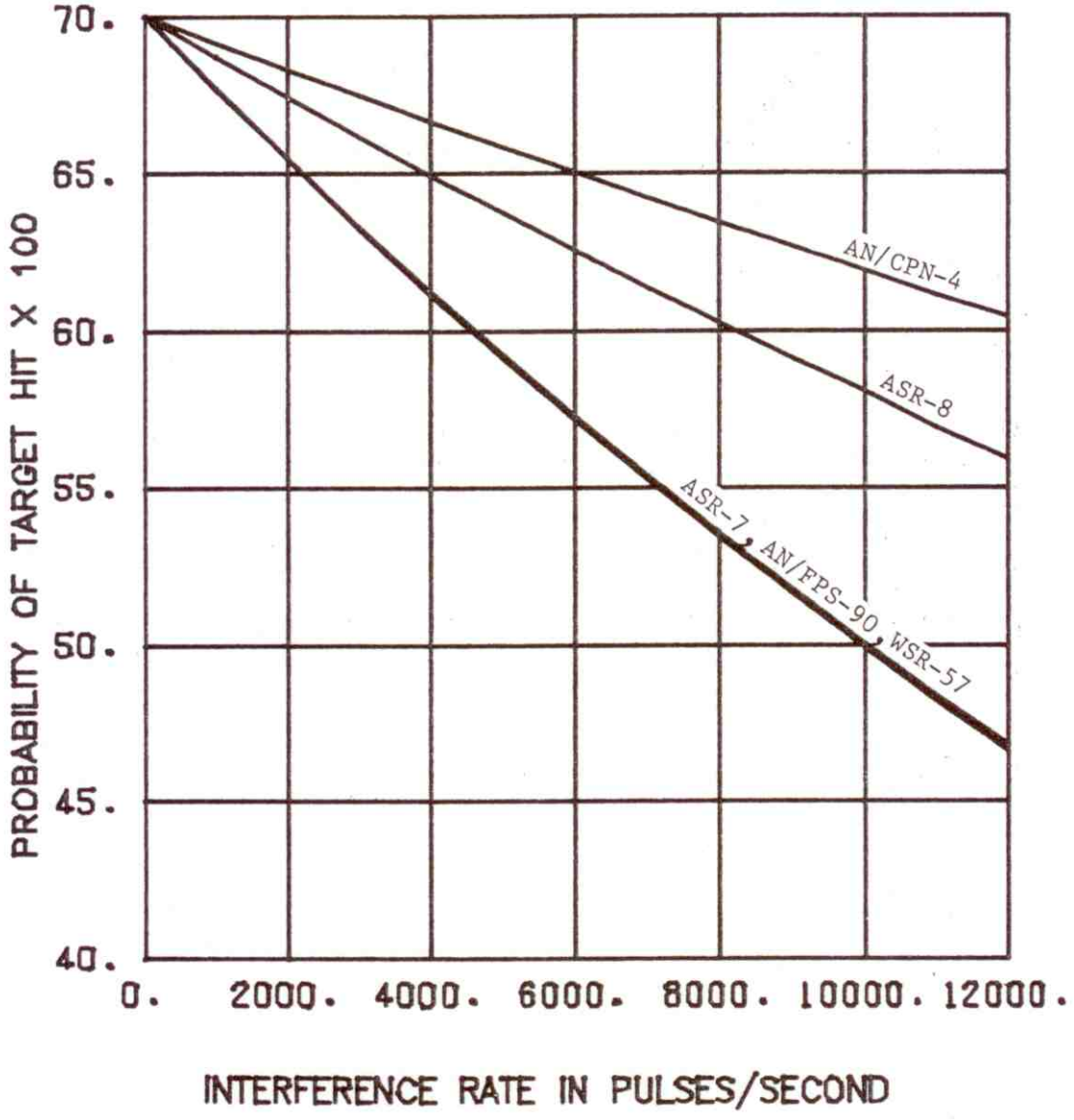

Figure 4-26. ARTS-IIIA/RDAS Probability of Target Hit Versus Rate of Received Interference (ASR-8 Victim Radar, MTI Channel, Rank Quantizer Threshold 23)

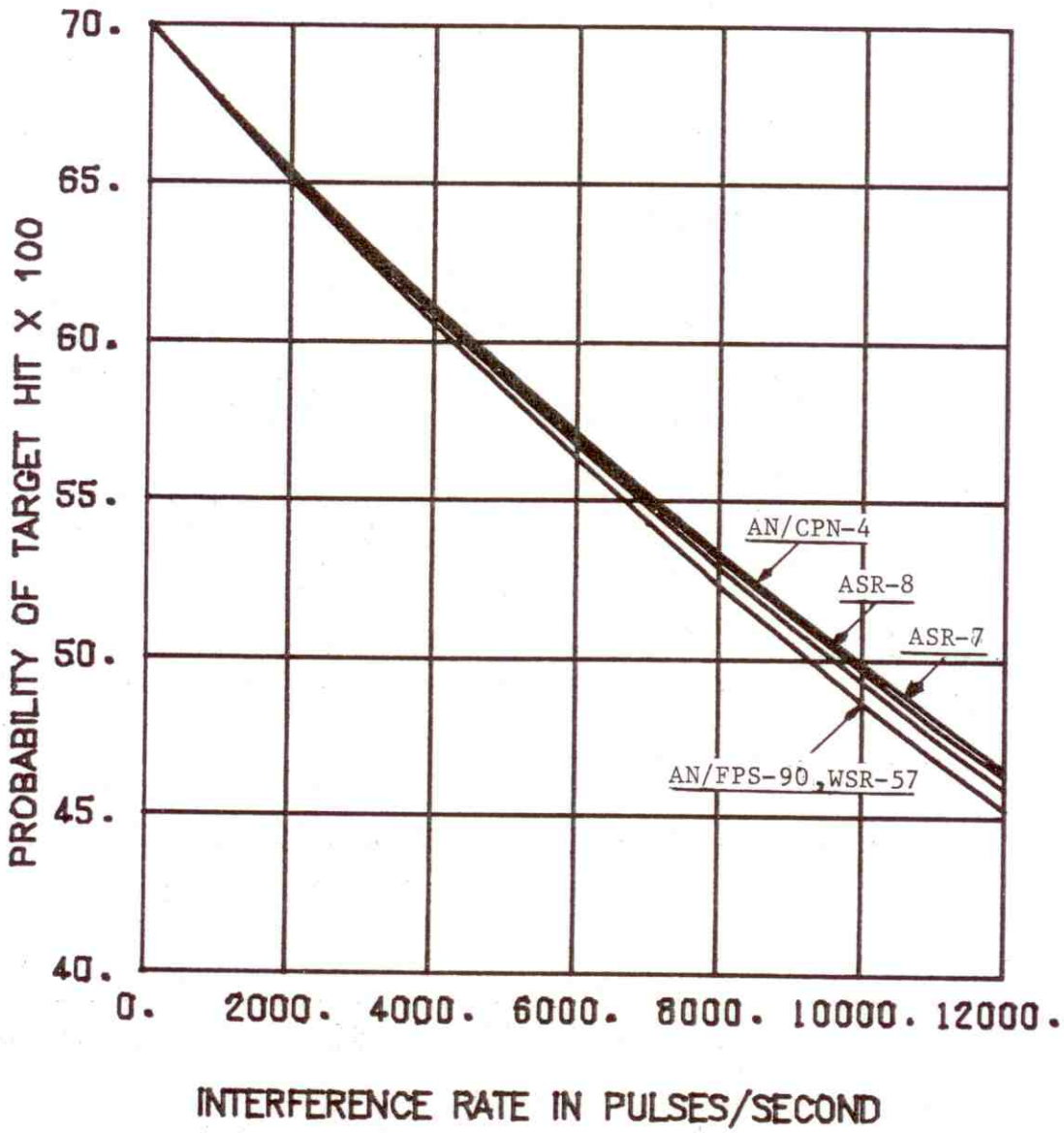

Figure 4-27. ARTS-IIIA/RDAS Probability of Target Hit Versus Rate of Received Interference (ASR-8 Victim Radar, MTI Channel, Rank Quantizer Threshold 24)

the ARTS-IIIA/RDAS interfaced to the ASR-7, and Figures 4-24 through 4-27 interfaced to the ASR-8. The graphs also account for the radar channel (normal or MTI) that is connected to the ARTS-IIIA/RDAS. The family of curves on each graph represent various interfering radar types. The even numbered graphs are for RQT=23 and the odd number graphs for RQT=24. The ν=0 value on each curve gives the probability of a target hit (0.7) without interference present. The same factors (interfering radar pulse width and PRF, and victim radar range bin characteristics) which affected the degree of interference impact on the probability of false target hit also applies to the probability of target hit. However, the probability of target hit decreased with interference, while in most cases the probability of a false target hit increased. This is because the probability of target hit (P_1 in Equation 4-1) is much greater than the probability of an interference pulse falling in the range bin of interest ($1-e^{-X_1\nu}$ in Equation 4-1). Under these conditions, Equation 4-1 can be approximated by:

$$P_{i1} = P_1 e^{-NX_2\nu} \qquad (4-19)$$

It is evident from this expression that the probability of hit can only decrease with increasing values of ν.

The data representing the curves in Figures 4-20 through 4-27 were reduced to the form shown in TABLES 4-8 through 4-11 to indicate the effect of a particular number and type of interfering radars on the probability of target hit. TABLES 4-8 and 4-9 represent data for an ARTS-IIIA/RDAS interfaced to an ASR-7 radar that is receiving interference from one and three radars, respectively. Similarly, TABLES 4-10 and 4-11 gives the probability of target hit when the ARTS-IIIA/RDAS is interfaced to an ASR-8 radar that is receiving interference. The interfering pulse arrival rate (ν) in TABLES 4-8 and 4-10 are simply equal to the average PRF of the interfering radar. In TABLES 4-9 and 4-11, ν is equal to three times the PRF of the interfering radar. The probability of target hit values listed in TABLES 4-8 through 4-11 indicate that connecting the ARTS-IIIA/RDAS to the MTI channel results in a lower probability of target hit than when connected to the normal channel. This is because N in Equation 4-19 is 3 for MTI and only 1 for normal channel. In other words, the probability of an interference pulse falling in a rank quantizer comparison range bin and precluding generation of a hit (logical 1) is greater for the MTI channel.

Interference Effect on Target Detection

The decision to declare a target is accomplished by the target detection software functions shown in Figure 4-5. The details of this target detection processing is given in the RDAS Subsystem Description section of this report. A computer program was written to determine the probability of target detection as a function of probability of target hit. The program involves

TABLE 4-8

ARTS-IIIA/RDAS PROBABILITY OF TARGET HIT WHEN CONNECTED TO ASR-7 RADAR THAT IS RECEIVING INTERFERENCE FORM ONE RADAR

VICTIM RADAR CHANNEL	INTERFERING RADAR	INTERFERING RATE ν PULSES/SEC	PROBABILITY OF TARGET HIT (RQT = 23)	PROBABILITY OF TARGET HIT (RQT = 24)
NORMAL	ASR-7	1002	0.6947	0.6893
NORMAL	ASR-8	1040	0.6981	0.6892
NORMAL	AN/CPN-4	1192	0.6996	0.6878
NORMAL	AN/FPS-90	356	0.6965	0.6962
NORMAL	WSR-57	166	0.6983	0.6981
MTI	ASR-7	1002	0.6842	0.6686
MTI	ASR-8	1040	0.6944	0.6681
MTI	AN/CPN-4	1192	0.6989	0.6641
MTI	AN/FPS-90	356	0.6897	0.6888
MTI	WSR-57	166	0.6949	0.6945

NOTE: RQT = RANK QUANTIZER THRESHOLD
PROBABILITY OF TARGET HIT WITHOUT INTERFERENCE = 0.7